

X-ray photoelectron spectroscopy characterization of gold nanoparticles functionalized with amine-terminated alkanethiols

Sirnegeda D. Techane, Lara J. Gamble, and David G. Castner^{a)}

National ESCA and Surface Analysis Center for Biomedical Problems, Departments of Chemical Engineering and Bioengineering, University of Washington Box 351750, Seattle, Washington 98195-1750, USA

(Received 27 May 2011; accepted 14 July 2011; published 18 August 2011)

Gold nanoparticles (AuNPs) functionalized with a short chain amine-terminated alkanethiol (HS-(CH₂)₂NH₂ or C2 NH₂-thiol) are prepared via a direct synthesis method and then ligand-exchanged with a long chain amine-terminated alkanethiol (HS-(CH₂)₁₁NH₂ or C11 NH₂-thiol). Transmission electron microscopy analysis showed the AuNPs were relatively spherical with a median diameter of 24.2 ± 4.3 nm. X-ray photoelectron spectroscopy was used to determine surface chemistry of the functionalized and purified AuNPs. The ligand-exchange process was monitored within the time range from 30 min to 61 days. By the fourth day of exchange all the C2 NH₂-thiol molecules had been replaced by C11 NH₂-thiol molecules. C11 NH₂-thiol molecules continued to be incorporated into the C11 NH₂ self-assembled monolayer between days 4 and 14 of ligand-exchange. As the length of the exchange time increased, the functionalized AuNPs became more stable against aggregation. The samples were purified by a centrifugation and resuspension method. The C2 NH₂ covered AuNPs aggregated immediately when purification was attempted. The C11 NH₂ covered AuNPs could be purified with minimal or no aggregation. Small amounts of unbound thiol (~15%) and oxidized sulfur (~20%) species were detected on the ligand-exchanged AuNPs. Some of the unbound thiol and all of the oxidized sulfur could be removed by treating the functionalized AuNPs with HCl. © 2011 American Vacuum Society. [DOI: 10.1116/1.3622481]

I. INTRODUCTION

The rapid increase in the use of nanoparticles in biotechnology applications has been driven by the unique properties of the nanomaterials provided by their high percentage of surface atoms.^{1–5} Size, shape and surface chemistry are all important properties for determining the performance of nanoparticles.⁶ By varying these properties one can tune the nanoparticle performance for a wide-range of applications.⁶ Special interest in gold nanoparticles (AuNPs) for *in vivo* nanomedicine studies can be attributed to their nontoxicity.^{7–9} AuNPs have also been used in areas such as microarray, biosensor, imaging, diagnostics, drug, and nucleic acid delivery, and fingerprinting applications.^{10–21} In these applications, the AuNPs are modified with surface ligands to allow subsequent biomolecule immobilization, or they are directly functionalized with the biomolecules. Among the common methods used to functionalize AuNPs is adsorbing a self-assembled monolayer (SAMs) of alkanethiols onto the AuNP surfaces.²² The preparation and characterization of SAMs on flat Au surfaces has been extensively studied for over three decades.^{22–36} Although SAMs are widely used to functionalize AuNPs, detailed, quantitative characterization of the SAM functionalized AuNPs is often lacking.⁴ For biomedical applications amine-terminated SAM functionalized AuNPs (NH₂-SAM-AuNPs) are commonly used as carriers to deliver immobilized biomolecules such as DNA and siRNA into cells, and to perform colorimetric assays of

enzymes such as hyaluronidase.^{37–39} Given the challenges of preparing well-defined, model amine SAMs on flat Au surfaces,⁴⁰ it is especially important to characterize NH₂-SAM-AuNPs.

AuNPs with diameters of ~5 nm, commonly known as monolayer protected clusters, have been successfully functionalized with amine-terminated ligands by including the amine thiol in the synthesis solution.^{41,42} However, it has been difficult to functionalize large AuNPs by ligand-exchange with NH₂-alkanethiols. We have observed that AuNPs with diameters >12 nm synthesized by the citrate reduction method^{43,44} aggregated severely and irreversibly when ligand-exchange of the citrate covered AuNPs was attempted with amine thiols. One-step ligand-exchange of the citrate covered AuNPs with OH and CH₃ terminated alkanethiols have also been shown to lead to aggregation.⁴⁵ A ligand-exchange method using thioctic acid and COOH-dithiol as an intermediate stabilizer and 11-amino-1-undecanethiol (C11 NH₂-thiol) as the final thiol was reported by Lin *et al.* to convert citrate-AuNPs to NH₂-SAM-AuNPs.⁴⁶ Though the two-step functionalization improved the stability of the AuNPs, the final AuNPs were not completely covered with the C11 NH₂-SAM.⁴⁶

Niidome *et al.* developed a one-step one-phase synthesis and functionalization of AuNPs (~34 nm diameter) with 2-aminoethanethiol (C2 NH₂-thiol).³⁷ Lee *et al.* reported using similar method to prepare 14 nm C2 NH₂-SAM-AuNPs.³⁸ These methods are a good starting point for preparing NH₂-SAM-AuNPs. However, the stability of functionalized AuNPs against aggregation typically depends on both the charge and chain length of the molecule used to functionalize the AuNPs.⁴⁵ For example, C2 NH₂-thiols are typically too short

^{a)} Author to whom correspondence should be addressed; electronic mail: castner@nb.uw.edu

to provide good AuNP stabilization against aggregation. Though Lee *et al.* reported purifying the C2 NH₂-SAM-AuNPs using dialysis,³⁸ we observed that using either dialysis or centrifugation for purification resulted in immediate aggregation of the C2 NH₂-SAM-AuNPs. Niidome *et al.* did not report if the NH₂-SAM-AuNPs were purified before DNA immobilization.³⁷ In another study, we found for AuNPs that shorter-chain COOH-SAMs provided less stabilization against aggregation than longer-chain COOH-SAMs.⁴⁷ Following similar reasoning, the short chain C2 NH₂-SAM is not expected to provide much stability against AuNP aggregation. Since surface characterization results such as x-ray photoelectron spectroscopy (XPS) were not reported in previous studies of C2 NH₂-SAM-AuNPs, the surface compositions and extent of purity of the C2 NH₂-SAM-AuNPs were unknown.

In the present study, we followed the method of Niidome *et al.*³⁷ to prepare C2 NH₂-SAM-AuNPs, but then performed a ligand-exchange to ultimately functionalize the AuNPs with C11 NH₂-SAMs. The AuNPs did not aggregate throughout the C2 to C11 amine thiol ligand-exchange process. Purification of the C11 NH₂-SAM-AuNPs, after the ligand-exchange, resulted in some aggregation of the AuNPs. This aggregation decreased with ligand-exchange time and it was completely reversed by adding few drops of 1M HCl. Transmission electron microscopy (TEM) was used to determine the size and shape of C2 NH₂-SAM-AuNPs, and XPS was used to determine surface chemistries of the AuNPs at various stages of the C11 amine thiol ligand-exchange process.

II. EXPERIMENT

A. Materials

The following chemicals were purchased from Sigma-Aldrich and used as received: gold (III) chloride hydrate (HAuCl₄ · xH₂O, x = ~3, 99.999%), cysteamine hydrochloride (HS-(CH₂)₂NH₂ · HCl, 98%), sodium borohydride (NaBH₄, 99%), and 11-amino-1-undecanethiol hydrochloride (HS-(CH₂)₁₁NH₂ · HCl, 99%). Additional reagents (company, concentration, and grade) included HCl (EMD Chemicals, Inc., 36.5–38%, ACS) and ethanol (AAPER, absolute 200 proof). Ultrapure water (resistivity >18.0 M Ω cm) was purified by a Modulab Analytical research grade water system. TEM grids (carbon type-A, 300 mesh, copper grids) were purchased from Ted Pella. Silicon wafers were purchased from Silicon Valley Microelectronics, diced into 0.6–1 cm × 1 cm pieces, then thoroughly cleaned by sonication in a series of organic solvents (dichloromethane, acetone and methanol; 2 × 5min consecutive treatments in each solvent). A CHA 600 electron beam evaporator was used to deposit 10 nm titanium films at pressures below 1 × 10⁻⁶ Torr onto the flat, clean silicon wafer pieces.

B. Synthesis of C₂ NH₂-SAM-AuNPs

The method developed by Niidome *et al.*³⁷ was used to synthesize the C2 NH₂-SAM-AuNPs. The main solutions were prepared as follows: 223.69 mg of HAuCl₄ was dissolved into

400 mL of ultrapure water to produce a 1.42 mM solution, 96.80 mg of cysteamine hydrochloride was dissolved into 400 μL of ultrapure water to produce a 213 mM solution, and 7.57 mg of NaBH₄ was dissolved into 20 mL of ultrapure water to produce a 10 mM stock solution. The HAuCl₄ solution was added to a 500 mL-plastic beaker, covered with a glass plate and aluminum foil, and then stirring with a magnetic bar was commenced. The cysteamine solution was added to the HAuCl₄ solution and the mixed solution was stirred for 20 min. Finally, 0.1 mL of the NaBH₄ solution was added and stirring was continued for 2 h. The final product was used immediately after synthesis for ligand-exchange with the C11 NH₂-thiol. Prior to the C11 NH₂-thiol exchange about 1 mL of the C2 NH₂-thiol sample was placed onto a TEM grid and allowed to air-dry on filter paper. This sample was then used for TEM analysis of the AuNP size and shape.

C. Ligand-exchange of C₂ NH₂-thiols with C11 NH₂-thiols on AuNPs

The C2 NH₂-SAM-AuNPs was ligand-exchanged with the C11 NH₂-thiol as follows. First, a 5 mM solution of the C11 NH₂-thiol was prepared in ethanol. Then, an excess amount of the thiol solution was added to the C2 NH₂-SAM-AuNPs solution in an aluminum foil covered flask. For example, 8 mL of a 5 mM C11 NH₂-thiol solution was added to a 400 mL of the C2 NH₂-SAM-AuNP solution. The mixture was then stirred on a magnetic plate. Samples (~30mL) were taken from the solution after the following times of ligand exchange: 30 min, 3 h, 12 h, 24 h, 2 days, 4 days, 7 days, 14 days, 21 days, 31 days, and 61 days.

Each of these samples were then divided into 20 1.5 mL microcentrifuge tubes and centrifuged at 10 000 RPM for 15 min at room temperature. After removing the supernatant, the precipitates were vortex-mixed and the contents from five tubes were combined into one tube. After adding ultrapure water and vortex-mixing, the samples were centrifuged again under the same conditions. Then, after removing the supernatant, the precipitates were vortex-mixed and the contents from two tubes were combined into one tube. Now, each sample was consolidated into two tubes and these tubes were further purified by repeating the centrifugation and vortex-mixing steps at least two times. Based on the XPS sulfur spectra, more rinsing was required for the longer ligand-exchange times to remove unbound thiols. Finally, the samples from the remaining two tubes were combined into a single tube and ~100 μL of ultrapure water was added to the tube. Then the sample was vortex-mixed to produce a homogeneous solution. An additional step involved addition of HCl acid. In this case, after finishing the purification stage, a different number of drops (1, 6, 12, and 24) of a 1M HCl solution was added to 4.8 mL of 24 × diluted purified/concentrated samples. Adding one drop of the HCl solution did not result in a noticeable change in amine covered AuNPs. Adding 6, 12, or 24 drops of the HCl solution resulted in similar noticeable changes in the amine covered AuNPs. These HCl treated samples were analyzed by XPS before and after rinsing with water.

For XPS analysis, a small drop ($\sim 20 \mu\text{L}$) of the final concentrated product was placed onto a clean titanium coated substrate and allowed to dry in a vacuum desiccator. This step was repeated until a complete layer of AuNPs was formed on the substrate and the substrate Ti signal was minimized during XPS analysis. The samples were stored in petri-dishes backfilled with nitrogen gas and wrapped with parafilm. XPS measurements were performed approximately two hours after the sample drying was completed.

D. Transmission electron microscopy

TEM measurements were performed on Philips CM100 instrument operating at 100 kV accelerating voltage. It was equipped with a Galan Model 689 digital slow scan camera. Pictures with 128×128 pixels were taken of the AuNPs with typical magnifications in the range of 90 000–340 000 \times . IMAGEJ software was used to analyze average diameter, size distribution and circularity of AuNPs from the TEM images. The results were based on analysis of approximately 1300 nanoparticles from three batches of C2 NH₂-SAM-AuNPs.

E. X-ray photoelectron spectroscopy

XPS measurements were performed on a Kratos AXIS Ultra DLD (Kratos, Manchester, UK) instrument in the “hybrid” mode using a monochromatic Al K α x-ray source and a nominal photoelectron take-off angle of 0° (the take-off angle is defined as the angle between the substrate normal and the axis of the analyzer lens). All samples were run as insulators using a low-energy flood gun for charge neutralization. For each sample, a survey scan from 0–1100 eV binding energy (BE) and elemental scans of N1s, O1s, S2p, and Ti2p were acquired using a pass energy of 80 eV on three spots to determine XPS compositions. High-resolution scans of C1s, N1s, S2p, and Au4f peaks were acquired from one spot on each sample using a 20 eV pass energy to examine the type of chemical species present. As a control, similar compositional measurements were acquired for the clean titanium substrates. Measurements were performed on three replicates for each sample. Data analysis was done using the Vision Processing data reduction software. All BEs were referenced to the C1s hydrocarbon peak at 285 eV.

III. RESULTS AND DISCUSSION

A. TEM analysis

A TEM image of the C2 NH₂-SAM-AuNPs is shown in Fig. 1. IMAGEJ analyses of the size and shape distributions based on 1300 nanoparticles are shown in Fig. 2. The median diameter and standard deviation of the AuNPs was 24.2 ± 4.3 nm. The circularity index of 72% of the AuNPs was less than 1.1, where circularity index was calculated as the ratio of major axis to minor axis of a nanoparticle.

B. XPS analysis

To prepare stable NH₂-SAM-AuNPs, a one-step synthesis and functionalization method was performed using C2 NH₂-

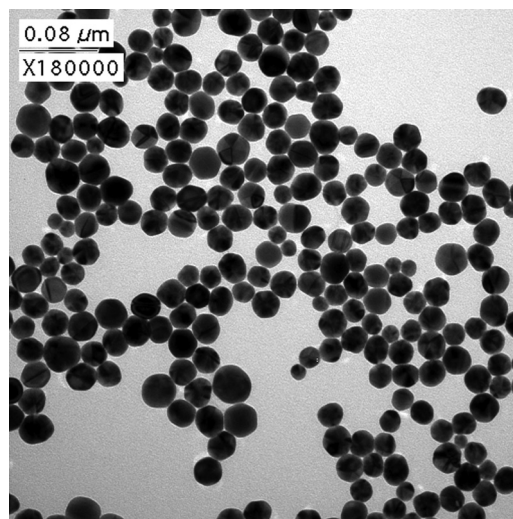


FIG. 1. TEM image of the C2 NH₂-SAM-AuNPs.

thiols followed by ligand exchange using C11 NH₂-thiols. We observed that the unpurified C2 NH₂-SAM-AuNPs were stable in solution for only a few days. When similar ligand exchange was performed on citrate-covered AuNPs or

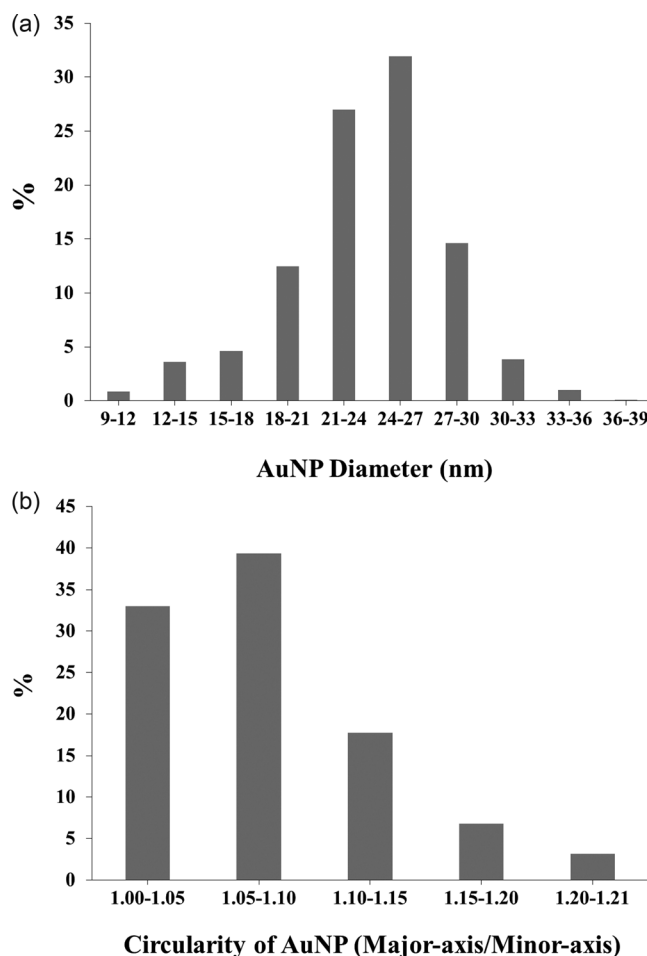


FIG. 2. IMAGEJ results for the size distribution (median diameter = 24.2 ± 4.3 nm) and circularity of C2 NH₂-SAM-AuNPs based on analysis of 1300 nanoparticles. The circularity is represented by the ratio of the major axis to the minor axis of a particle.

TABLE I. XPS determined compositions of the NH₂-SAMs on 24 nm AuNPs after undergoing a C11 NH₂-thiol ligand-exchange with a C2 NH₂-SAM for different lengths of time (30 min to 61 days). The data was normalized without the Ti signal as discussed in the text.

Time of ligand-exchange	at. % (std. dev.)				
	C1s	Au4f	N1s	O1s	S2p
30 min	23.6(3.8)	64.6(3.1)	5.3(0.8)	2.2(0.5)	4.4(0.4)
3 h	23.5(2.6)	63.7(2.4)	5.4(0.8)	2.3(0.4)	4.4(0.5)
12 h	25.9(3.7)	61.9(3.6)	5.4(0.8)	2.3(0.3)	4.5(0.4)
24 h	27.3(7.6)	56.8(6.0)	4.2(1.0)	2.6(0.4)	4.0(0.5)
2 days	36.2(5.1)	52.5(4.8)	4.5(0.4)	2.8(0.3)	4.0(0.3)
4 days	43.9(3.9)	45.7(4.1)	4.0(0.4)	2.4(0.3)	4.0(0.2)
7 days	47.5(4.2)	42.3(4.0)	4.2(0.5)	2.1(0.3)	3.9(0.4)
14 days	51.3(2.6)	37.0(2.9)	4.6(0.4)	2.9(0.5)	3.9(0.3)
21 days	51.6(1.2)	36.4(0.9)	4.7(0.4)	3.5(0.6)	3.6(0.4)
31 days	50.6(1.5)	36.9(1.3)	4.8(0.4)	3.6(0.1)	3.8(0.3)
61 days	52.3(1.5)	35.5(1.1)	4.8(0.3)	3.3(0.5)	3.9(0.3)

AuNPs that had been functionalized with C6 COOH-SAMs (mercaptohexanoic acid SAMs), the AuNP aggregated irreversibly. This could be due to reversal of the surface charge from the negatively charged citrate or COOH-SAM covered AuNPs to the positively charged NH₂-SAM covered AuNPs. Therefore, it appears to be advantageous to have the same surface functionalities on the AuNP surfaces before and after the exchange with the final ligand. Our results indicate that this prevents aggregation of the amine functionalized AuNPs during final functionalization step.

Composition results from XPS analysis of the NH₂-SAM-AuNPs after various ligand-exchange times are compiled in Table I. All samples showed the presence C, N, and S from the NH₂-SAMs overlayer, as well as Au from the NPs. In addition to these expected elements, O was detected. Previously it has been reported that oxygen is a common contaminant observed on NH₂-SAMs formed on flat Au surfaces.^{40,48,49} Small amounts of Ti from the underlying Ti coated substrate were also observed on some of the samples. The Ti atomic concentrations for those samples were as follows at the various ligand-exchange times: 0.2% (3 h), 1.5% (24 h) and 0.1% (14, 21, and 31 days). To remove the contributions from the Ti substrate, proportional values from the measured composition of a bare Ti surface (at. %: Ti = 30.2, O = 40.6, C = 21.0, and N = 2.3) were subtracted from the NH₂-SAM-AuNP samples, and the data was then renormalized.

As shown in Table I, the C concentration increased from ~24 at. % to ~52% while the Au concentration correspondingly decreased from ~65% to ~35 at. % (an increase of the C/Au atomic ratio from 0.4 to 1.5) when the ligand-exchange was increased from 30 min to 61 days. The changes in the C and Au signals with ligand-exchange time are consistent with increasing replacement of the shorter C2 NH₂-thiol molecules with the longer C11 NH₂-thiol molecules. The C11 NH₂ SAM contains more carbon atoms and the resulting thicker SAM attenuates the Au signal more.⁵⁰ As shown in Table I, the N concentration also decreased slightly with

increased ligand-exchange time. The shortest ligand-exchange times had the highest N concentration, while the longest ligand-exchange times had the lowest N concentration. The N/C atomic ratio, as well as the S/C atomic ratio, decreased from 0.2 to 0.1 when ligand-exchange time increased from 30 min to 61 days. These results are consistent with more C2 NH₂-thiols on the AuNPs at shorter exchange times and more C11 NH₂-thiols on the AuNPs at longer exchange times as the relative concentrations of N and S are higher in the C2 NH₂-thiol than in the C11 NH₂-thiol. The O concentration increased slightly with time. While it has been shown that oxygen-containing contaminants are present in amine SAMs,⁴⁰ high-resolution XPS S2p spectra showed that some of the detected oxygen from the NH₂-SAM-AuNP samples was associated with the presence of oxidized sulfur, as discussed below.

In Fig. 3 the surface compositions of just the SAM overlayers, renormalized without the Au and O concentrations, were compared with the stoichiometric compositions of the two thiols to examine the replacement of the C2 NH₂-thiol with the C11 NH₂-thiol. The carbon concentration increases, while both the nitrogen and sulfur concentrations decrease with increasing ligand exchange time. At first time point the carbon concentration is higher and the nitrogen and sulfur concentrations lower than those expected for a pure C2 NH₂-thiol. This indicates a significant amount of the C2 NH₂-thiol is already replaced by C11 NH₂-thiol within the first 30 min of ligand-exchange. The composition of the C2 NH₂ covered AuNPs before ligand exchange could not be measured since this sample immediately aggregated upon trying to purify it for analysis. As the ligand-exchange is increased to 4 days and beyond, the renormalized composition of C, N, and S became constant and the error bars decreased, showing that the sample compositions became more reproducible. The measured C, N, and S concentrations at exchange times longer than 4 days are consistent with the presence of a fully exchanged C11 NH₂-SAM on the AuNPs. However, the data before renormalization indicates that the sample composition continues to change until 14 days of exchange time. Most notably the Au atomic percentage continued to decrease until 14 days, indicating the Au signal is increasingly attenuated by further changes in the SAM overlayer. This suggests a mechanism where during the first 4 days of exchange the C11 NH₂-thiols have completely replaced the C2 NH₂-thiols on the surface of the AuNPs, then from 4 to 14 days of exchange additional C11 NH₂-thiols are incorporated in the SAM. This second step would result in a more densely packed SAM that would further attenuate the Au signal from the NP core.

Figure 4 shows representative XPS high-resolution C1s and N1s spectra from the 21-day, ligand-exchanged NH₂-SAM-AuNPs. The C1s spectrum has two peaks. One peak has a BE of 285.0 eV (C–H and C–C) and the other peak has a BE of 286.6 eV (C–N and C–S), with each peak containing approximately 87 and 13% of the total C1s intensity, respectively. These results are comparable with those found for the C11-NH₂ SAM on flat gold surfaces.⁴⁰ The N1s spectrum

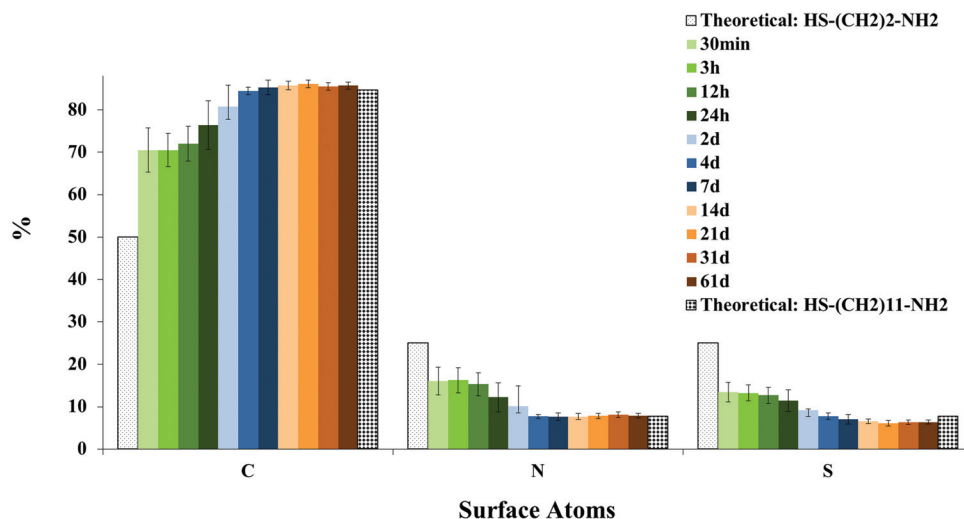


FIG. 3. (Color) XPS determined compositions of NH_2 -SAMs on the 24 nm AuNP surface after undergoing a C11 NH_2 -thiol ligand-exchange for different lengths of time (30 min to 61 days). The theoretical stoichiometric compositions for the C2 NH_2 -thiol and C11 NH_{11} -thiol are also shown. The experimental data was renormalized without the Au, O, and Ti signals as discussed in the text.

contained two peaks at 399.8 eV ($\text{NH}_2\text{-C}$) and 401.2 eV ($^+\text{NH}_3\text{-C}$). In Fig. 4(b) these peaks have intensities that are 40 and 60% of the total $\text{N}1s$ intensity, respectively. The intensity ratio between the two $\text{N}1s$ peaks was not consistent,

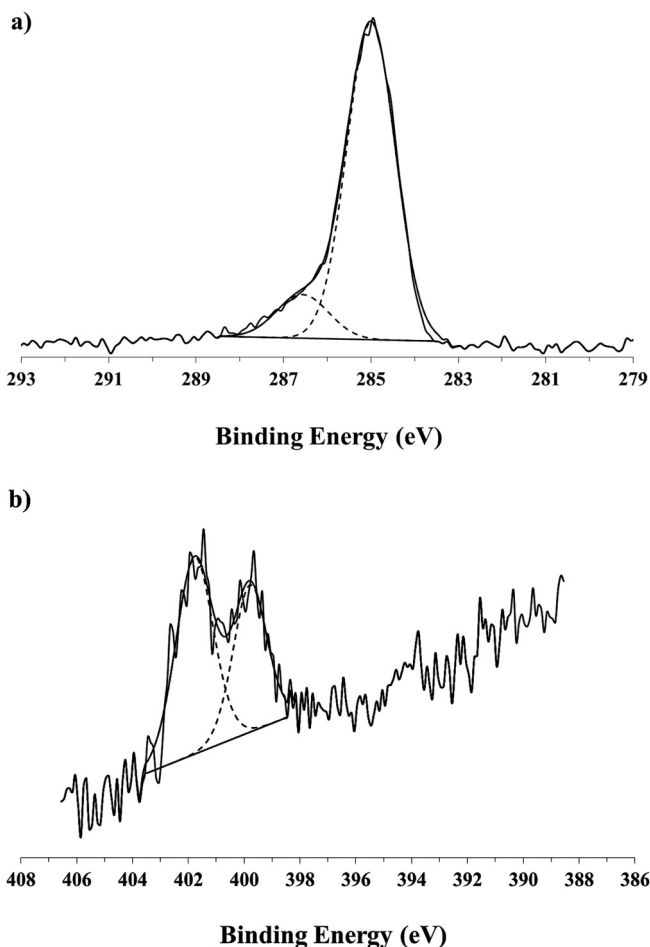


FIG. 4. XPS high-resolution spectra of (a) $\text{C}1s$ and (b) $\text{N}1s$ for NH_2 -SAMs on 24 nm AuNPs after 21 days of ligand-exchange.

even for different replicates of the same samples likely due to lack of potential control as the samples are removed from solution. Similar results been reported for the C11- NH_2 SAM on flat gold surfaces.⁴⁰

Figure 5(a) shows a representative XPS high-resolution $\text{S}2p$ spectrum from the 21-day, ligand-exchanged NH_2 -SAM-AuNPs. The $\text{S}2p$ peaks were fit using doublet peaks with a $2p_{1/2}/2p_{3/2}$ ratio of 0.5 and separation of 1.2 eV, as described previously.³² The spectrum in Fig. 5(a) contained three sets of doublets. The most intense doublet is attributed to a surface bound Au-thiolate species (162 eV $\text{S}2p_{3/2}$ BE).³² The two smaller doublets are attributed to unbound thiols ($\text{S}2p_{3/2}$ BE near 163.5 eV) and oxidized sulfur ($\text{S}2p_{3/2}$ BE near 168 eV).³² Typically it was observed in most samples that ~ 65 , 10–20, and 15–20% of sulfur atoms were present as bound Au-thiols, unbound thiols and oxidized sulfur species, respectively. The typical spectrum shown here in Fig. 5(a) had 67% bound Au-thiolate, 16% unbound thiol, and 17% oxidized S.

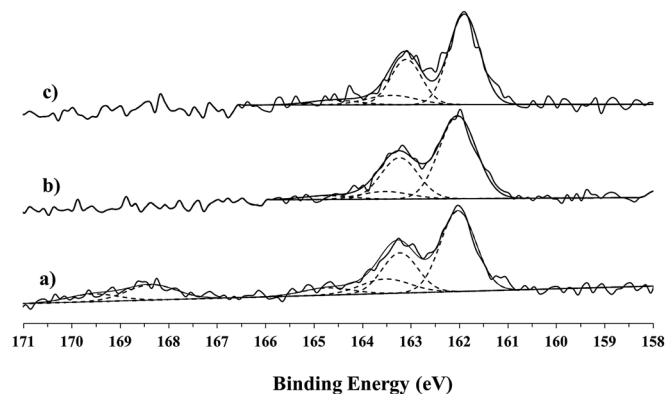


FIG. 5. XPS high-resolution $\text{S}2p$ spectra from NH_2 -SAMs on 24 nm AuNPs that were purified after 21 days of ligand-exchange for samples analyzed—(a) before adding HCl, (b) after adding 24 drops of the HCl solution but before rinsing, and (c) after adding 24 drops of the HCl solution and rinsing.

TABLE II. XPS determined compositions of NH₂-SAMs on 24 nm AuNPs after undergoing a C11 NH₂-thiol ligand-exchange with a C2 NH₂-SAM for 21 days followed by purification (before adding HCl), purification then adding 24 drops of HCl solution (with HCl), or purification then adding 24 drops of HCl solution and rinsing (after rinsing HCl). Data for the sample with the unrinsed acid treatment was renormalized without the Cl signals.

21 days ligand-exchanged	at. % (std. dev.)				
	C1s	Au4f	N1s	O1s	S2p
Before adding HCl	51.6(1.2)	36.4(0.9)	4.7(0.4)	3.5(0.6)	3.6(0.4)
With HCl	51.5(1.2)	39.7(1.1)	4.8(0.3)	1.3(0.1)	2.8(0.2)
After rinsing HCl	54.8(1.4)	36.0(2.0)	4.8(0.4)	1.4(0.6)	2.7(0.2)

An additional HCl treatment was done to better disperse the nanoparticles. A comparison of the XPS data before and after treatment with 24 drops of the HCl solution showed that the addition of HCl also resulted in the removal of some of the unbound thiol and all of the oxidized sulfur. The 21-day, ligand-exchanged NH₂-SAM-AuNPs had ~7% unbound thiols after HCl treatment and ~11% unbound thiols after rinsing the HCl treated samples. However, oxidized sulfur was not detected on the samples treated with HCl, even if the acid treatment was followed by a final rinsing step. Figure 5(b) and 5(c) show representative high-resolution XPS S2p spectra after the addition of 24 drops of the HCl solution to the NH₂-SAM-AuNP solution. The rinsing was performed by centrifuging the sample under the conditions noted in the experimental section with a 3 × water change. To remove more of the unbound thiol species, additional steps of centrifugation, rinsing in the presence of HCl to prevent aggregation, then final rinsing to remove the HCl is recommended. The surface compositions of the three types of samples (before adding HCl, after adding HCl, and after adding HCl and then rinsing) are shown in Table II. A contribution from Cl of 3–4 at. % was observed on samples that were treated with HCl and not rinsed. Cl was not detected after the final rinsing with water. The surface composition of the “with HCl” sample shown in Table II has been renormalized without the Cl contribution to better compare the composition of that sample to the compositions of the “before HCl” and “after rinsing” samples. As seen in Table II, the O1s concentration decreased from 3.5 at. % (before HCl) to 1.4 at. % (after rinsing). The amount of sulfur also decreased from 3.6 to 2.7 at. % after the HCl treatment and a final rinse. These results are consistent with the removal of the oxidized sulfur species. Interestingly, the Au, N, and C percentages are not significantly changed after the HCl treatment and rinsing. This may indicate that the oxidized sulfur species removed was a sulfate ion and not an oxidized amine thiol molecule.

The XPS results reported in this study are the first step to preparing well-defined and well-characterized AuNPs covered with amine SAMs. Further studies to obtain more detail about the SAM thickness and structure on AuNPs can be obtained using by combining simulated electron spectra for surface analysis calculations with the experimental XPS measurements.⁵¹ Time-of-flight secondary ion mass spec-

trometry can provide additional structural insights into SAM covered AuNPs.⁴⁷ Additional complementary analysis techniques such as sum frequency generation vibration spectroscopy can provide further information such as the density of gauche defects in the alkyl chains as well as the orientation of those chains.⁴⁰

IV. CONCLUSIONS

C11 NH₂-SAM-AuNPs were prepared by starting with a previously reported one-step C2 NH₂-SAM-AuNPs synthesis/functionalization method followed by a ligand-exchange to replace the C2 NH₂-thiol molecules with C11 NH₂-thiol molecules. TEM showed the starting C2 NH₂-SAM-AuNPs were relatively spherical and reasonably monodispersed (average diameter of 24.2 ± 4.3 nm). The C11 NH₂-SAM-AuNPs were more stable than the C2 NH₂-SAM-AuNPs, which exhibited significant aggregation during attempts to purify them. The C11 NH₂-SAM-AuNPs could be purified with a centrifugation/resuspending method. XPS analysis showed that by day 4 of exchange most of the shorter C2 NH₂-thiol molecules were replaced by the longer C11 NH₂-thiol molecules. However, the longer thiols continued to be incorporated into the SAM until day 14 of exchange. XPS results detected the presence of bound, unbound, and oxidized sulfur species. Partial removal of the unbound thiol molecules and complete removal of the oxidized sulfur species was achieved with treatment of the samples with HCl. The final C11 NH₂-SAM-AuNPs are stable nanoparticles that can be used as a model surfaces for biomolecule immobilization.

ACKNOWLEDGMENTS

This research was supported by NIH Grants Nos. GM-074511 and EB-002027 (NESAC/Bio). S.D.T. thanks NSF for an IGERT fellowship.

- ¹D. Pissuwan, T. Niidome, and M.B.J. Cortie, *J. Controlled Release* **149**, 65 (2011).
- ²E. Katz and I. Willner, *Angew. Chem., Int. Ed. Engl.* **43**, 6042 (2004).
- ³C. S. S. R. Kumar, *Nanotechnologies for the Life Sciences*, 1st ed. (Wiley-VCH Verlag, Weinheim, 2005).
- ⁴D. W. Grainger and D. G. Castner, *Adv. Mater.* **20**, 867 (2008).
- ⁵D. R. Baer, D. J. Gaspar, P. Nachimuthu, S. D. Techane, and D. G. Castner, *Anal. Bioanal. Chem.* **396**, 983 (2010).
- ⁶M.-C. Daniel and A. Didier, *Chem. Rev.* **104**, 293 (2004).
- ⁷I. H. El-Sayed, X. Huang, and M. A. El-Sayed, *Nano Lett.* **5**, 829 (2005).
- ⁸S. Eustis and M. A. El-Sayed, *Chem. Soc. Rev.* **35**, 209 (2006).
- ⁹P. K. Jain, K. S. Lee, I. H. El-Sayed, and M. A. El-Sayed, *J. Phys. Chem. B* **110**, 7238 (2006).
- ¹⁰Z. Wang, J. Lee, A. R. Cossins, and M. Brust, *Anal. Chem.* **77**, 5770 (2005).
- ¹¹T. A. Taton, G. Lu, and C. A. Mirkin, *J. Am. Chem. Soc.* **123**, 5164 (2001).
- ¹²T. A. Taton, C. A. Mirkin, and R. L. Letsinger, *Science* **289**, 1757 (2000).
- ¹³K. Sokolov, M. Follen, J. Aaron, I. Pavlova, A. Malpica, R. Lotan, and R. Richards-Kortum, *Cancer Res.* **63**, 1999 (2003).
- ¹⁴D. Shenoy, W. Fu, J. Li, C. Crasto, G. Jones, C. DiMarzio, S. Sridhar, and M. Amiji, *Int. J. Nanomedicine* **1**, 51 (2006).
- ¹⁵C. A. Mirkin, R. L. Letsinger, R. C. Mucic, and J. J. Storhoff, *Nature (London)* **382**, 607 (1996).
- ¹⁶R. Leggett, E. E. Lee-Smith, S. M. Jickells, and D. A. Russell, *Angew. Chem., Int. Ed.* **46**, 4100 (2007).
- ¹⁷J.-S. Lee, S. I. Stoeva, and C. A. Mirkin, *J. Am. Chem. Soc.* **128**, 8899 (2006).

- ¹⁸J. M. Bergen, H. A. von Recum, T. T. Goodman, A. P. Massey, and S. H. Pun, *Macromol. Biosci.* **6**, 506 (2006).
- ¹⁹K. Aslan, J. R. Lakowicz, and C. D. Geddes, *Anal. Chem.* **77**, 2007 (2005).
- ²⁰K. Aslan, C. C. Luhrs, and V. H. Perez-Luna, *J. Phys. Chem. B* **108**, 15631 (2004).
- ²¹A. P. Alivisatos, K. P. Johnsson, X. Peng, T. E. Wilson, C. J. Loweth, M. P. Bruchez, Jr., and P. G. Schultz, *Nature (London)* **382**, 609 (1996).
- ²²J. C. Love, L. A. Estroff, J. K. Kriebel, R. G. Nuzzo, and G. M. Whitesides, *Chem. Rev.* **105**, 1103 (2005).
- ²³R. G. Nuzzo and D. L. J. Allara, *Am. Chem. Soc.* **105**, 4481 (1983).
- ²⁴T. J. Lenk, V. M. Hallmark, C. L. Hoffman, J. F. Rabolt, D. G. Castner, C. Erdelen, and H. Ringsdorf, *Langmuir* **10**, 4610 (1994).
- ²⁵L. Strong and G. M. Whitesides, *Langmuir* **4**, 546 (1988).
- ²⁶C. D. Bain, E. B. Troughton, Y. T. Tao, J. Evall, G. M. Whitesides, and R. G. J. Nuzzo, *Am. Chem. Soc.* **111**, 321 (1989).
- ²⁷M.-W. Tsao, C. L. Hoffman, J. F. Rabolt, H. E. Johnson, D. G. Castner, C. Erdelen, and H. Ringsdorf, *Langmuir* **13**, 4317 (1997).
- ²⁸L. H. Dubois and R. G. Nuzzo, *Annu. Rev. Phys. Chem.* **43**, 437 (1992).
- ²⁹S. Pan, D. G. Castner, and B. D. Ratner, *Langmuir* **14**, 3545 (1998).
- ³⁰A. Ulman, *Chem. Rev.* **96**, 1533 (1996).
- ³¹D. J. Graham and B. D. Ratner, *Langmuir* **18**, 5861 (2002).
- ³²D. G. Castner, K. Hinds, and D. W. Grainger, *Langmuir* **12**, 5083 (1996).
- ³³F. Tao and S. L. Bernasek, *Chem. Rev.* **107**, 1408 (2007).
- ³⁴F. Cheng, L. J. Gamble, and D. G. Castner, *Anal. Chem.* **80**, 2564 (2008).
- ³⁵C.-Y. Lee, P. Gong, G. M. Harbers, D. W. Grainger, D. G. Castner, and L. J. Gamble, *Anal. Chem.* **78**, 3316 (2006).
- ³⁶N. Xia, Y. Hu, D. W. Grainger, and D. G. Castner, *Langmuir* **18**, 3255 (2002).
- ³⁷T. Niidome, K. Nakashima, H. Takahashi, and Y. Niidome, *Chem. Commun.* **17**, 1978 (2004).
- ³⁸S. H. Lee, K. H. Bae, S. H. Kim, K. R. Lee, and T. G. Park, *Int. J. Pharm.* **364**, 94 (2008).
- ³⁹J.-W. Kim, J. H. Kim, S. J. Chung, and B. H. Chung, *Analyst (Cambridge, U. K.)* **134**, 1291 (2009).
- ⁴⁰J. E. Baio, T. Weidner, J. Brison, D. J. Graham, L. J. Gamble, and D. G. Castner, *J. Electron Spectrosc. Relat. Phenom.* **172**, 2 (2009).
- ⁴¹A. C. Templeton, M. J. Hostetler, E. K. Warmoth, S. Chen, C. M. Hartshorn, V. M. Krishnamurthy, M. D. E. Forbes, and R. W. Murray, *J. Am. Chem. Soc.* **120**, 4845 (1998).
- ⁴²E. C. Cutler, E. Lundin, B. D. Garabato, D. Choi, and Y.-S. Shon, *Mater. Res. Bull.* **42**, 1178 (2007).
- ⁴³J. Turkevich, P. C. Stevenson, and J. Hillier, *Discuss. Faraday Soc.* **11**, 55 (1951).
- ⁴⁴G. Frens, *Nature (London)* **241**, 20 (1973).
- ⁴⁵C. S. Weisbecker, M. V. Merritt, and G. M. Whitesides, *Langmuir* **12**, 3763 (1996).
- ⁴⁶S.-Y. Lin, Y.-T. Tsai, C.-C. Chen, C.-M. Lin, and C. -H. Chen, *J. Phys. Chem. B* **108**, 2134 (2004).
- ⁴⁷S. D. Techane, L. J. Gamble, and D. G. Castner, *J. Phys. Chem. C* **115**, 9432 (2011).
- ⁴⁸H. Wang, S. Chen, and L. Li, and S. Jiang, *Langmuir* **21**, 2633 (2005).
- ⁴⁹H. Wang, D. G. Castner, B. D. Ratner, and S. Jiang, *Langmuir* **20**, 1877 (2004).
- ⁵⁰B. D. Ratner and D. G. Castner, "Electron Spectroscopy for Chemical Analysis", 2nd ed., edited by J. C. V. Gilmore (Wiley, Chichester, 2009), pp 47–112.
- ⁵¹S. D. Techane, D. R. Baer, and D. G. Castner, "Simulation and Modeling of Self-Assembled Monolayers of Carboxylic Acid Thiols on Flat and Nanoparticle Gold Surfaces," *Anal. Chem.* (in press).